Computerised Image-Processing System for Fission-Track Dating : System Configuration and Functions

Title	Computerised Image-Processing System for Fission-Track Dating : System Configuration and Functions
Author	Wadatsumi, Kiyoshi / Masumoto, Shinji / Suzuki, Kazuyo
Citation	Journal of geosciences Osaka City University 31; 19-46.
Issue Date	1988-03
ISSN	0449-2560
Type	Departmental Bulletin Paper
Textversion	Publisher
Publisher	Faculty of Science, Osaka City University
Description	

Computerized Image-Processing System for Fission-Track Dating; System Configuration and Functions

Kiyoshi Wadatsumi, Shinji Masumoto and Kazuyo Suzuki

(With 36 Figures and 5 Tables)

Abstract

A computerized image-processing system for fission-track dating (CIPS-FTD) has been developed. The fundamental configuration of the system is similar to the system reported at the international FTD workshop in New York, 1984 (Wadatsumi and Masumoto, 1984), except for the new optical laser disk controller with a changeable cartridge (1.2 Giga-bytes per each volume) that makes it possible to develop the image-database. One of the difficulties with the system is that it requires enormous memory spaces. However it became possible to measure three-dimensional FT patterns with the image-database.

In order to develop the programs for FT dating, it was necessary to analyze both the general experimental procedures and the man-machine interactive operations. This means that software developers require either knowledge of general FT dating or experience of computer system development. Though specialized systems for application to artificial intelligence still contain many difficulties, these were overcome to develop this system as a man-machine interactive system by which the user's intelligence becomes effective. Therefore, users of the system only need general knowledge and techniques for FT dating, but no knowledge of either design or programming of the computerized system. The procedural technique for FT dating using the CIPS-FTD has been arranged in a flow chart which combines both the external detector method and the re-etching method for the external and internal faces.

The applicable functions of the CIPS-FTD in this procedure have resulted in a very powerful technology for a variety of operations. These are as follows; (a) procedural modeling and logical structure in the image-database, (b) the registration of samples and grains, (c) evaluation of etching conditions, (d) the measurement of the three-dimensional FT patterns, (e) the measurement of induced FTs in the re-eched grain, (f) the measurement of induced FTs in the external detector, and (g) the calculation and display of the results.

Many of the automatic operations realized in the measurement procedures make performance very high, but overall time for FT dating by the system is about one to three times that of the usual way. Thus, the system would be evaluated lower than if it only obtained the age of a sample. However, the system is valuable from another point of view, that the system measures not only the FT ages of a sample but also the three-dimensional patterns of FTs.

The most valuable aspect of the system is that it can permanently preserve a series of data from the unprocessed raw digital pictures to the final numerical values of results. All of this data can be obtained and used for checking, deleting, adding and replacing at any time or at any processing point in FT dating. Because of those functions of the system, the experimental techniques and results, which are often closed and unavailable to the public, could be opened to all who want to know more about and test the results of FT dating.

In the future, papers will be presented in which the zeta calibration values and the description of the three-dimensional FT patterns with reference to the age standards are discussed.

1. Introduction

(1) *Design Problems in a Computerized System*

Experiments in fission-track (FT) dating have provided us with very useful and important information in a variety of microscopic FT images. Effective utilization of this data requires considerable analysis. Recent demands for technology in FT dating to measure three-dimensional FT patterns (location, real length and direction) have brought rapid increases both in the number of these images and in the complexity of analysis, so that it is now inefficient or impossible for people to examine this data. Consequently, it is highly desirable to develop an integrated system which handles a variety of FT images with the aid of a computer. We have devoted our efforts to developing a computerized image-processing system for FT dating (CIPS-FTD). The strategies for it's development are as follows:

(a) The target of development has been the construction of a special system for very limited application to FT dating by designing man-machine systems to handle, store, and analyze the FT image-data.

(b) A wide variety of scientists in geochronology, including persons who are unfamiliar with computer programming, can communicate easily with the systems in an interactive mode.

(c) Because of the large amount of data, the system searches a set of image-data to examine, analyze and convert them into compact, well structured information for easy, quick, inexpensive storage and access. In order to realize these functions, an image-database should be used.

(d) Through interactive operations, user's knowledge of the images and objects can be fully utilized to generate and update models of the three-dimensional FT patterns. These models are very useful for the efficient and accurate analysis of FT image-data.

(2) *Problems in the Application of the CIPS-FTD*

Consideration of application problems related to the system forces us to consider the kind of difficulties that lie in experimental procedures and how to solve them by means of the system. Many factors which influence the efficiency of revealing FT make the experimental procedures difficult and erroneous. Such factors are as follows; (a) material differences in the samples and external detectors, (b) geometric factors, (c) crystallographic orientation, (d) inhomogeneous distribution of uranium, (e) fading and annealing, (f) FT etching conditions, and (g) criteria for FT identification.

Those difficulties have led to the development of several procedural techniques for FT dating (Hurford and Green, 1982). Among them, the external track detector method has been widely accepted by researchers in the FT dating community. The external track detector method has the following advantages; (a) it is not necessary to erase the spontaneous FTs in the sample by annealing, (b) grain-by-grain age determination is acceptable for small single grains with higher and varying uranium contents. On the other hand, the disadvantages lie in the necessity to correct the difference in the efficiency

which is caused by material or geometrical differences between samples and detectors, and in the difficulty in evaluating thermal fading based upon the length comparisons between spontaneous and induced FTs.

Recently, it has been recognizing that stability in the natural and experimental annealing of FTs in the external face of a sample is likely to be much more stable than that in the internal face, so that the difference between the ages of the external/internal faces in an annealed sample could be expected (WATANABE and ISHIBASHI, 1987).

In order to solve the difficulties described above, the procedural technique for FT dating using the CIPS-FTD has been arranged in a flow chart combining both the external detector method and the re-etching method for the external and internal faces, as shown in Fig. 1. The applicable functions of the CIPS-FTD in this procedure have provided us with a very powerful technology in a variety of operations. These are as follows; (a) procedural modeling and logical structure in the image-database, (b) registration of samples and grains, (c) evaluation of the etching condition, (d) measurement of
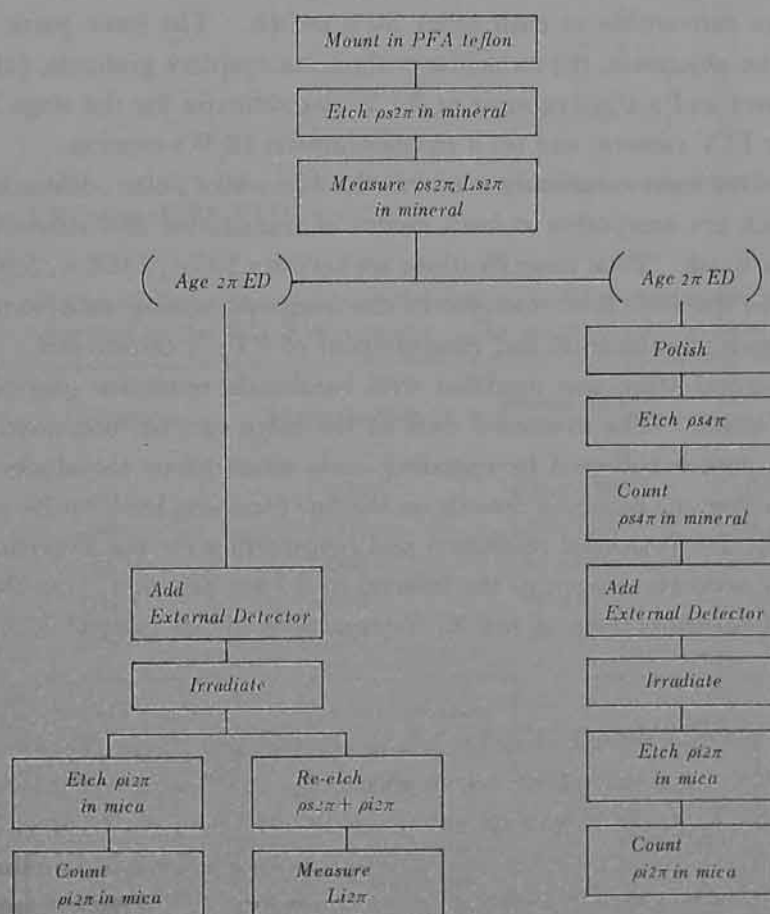

Fig. 1. A flow chart of procedural techniques for FT dating by the computerized image-processing system (CIPS-FTD), which combine both the external detector method and the re-etch method for the external and internal faces.

the three-dimensional FT patterns, (e) measurement of induced FTs in the re-etched grain, (f) measurement of induced FTs in the external detector, and (g) calculation and display of the results.

In this paper, we mainly present the system configuration and the applicable functions of the CIPS-FTD. The results from calibration of the CIPS-FTD using age standards, such as the Fish Canyon Tuff zircon and apatite, will be presented in the future.

2. System Description

The CIPS-FTD consists mainly of four units; (1) the microscope and the ITV camera subsystem, (2) the image-processing subsystem, (3) the image-database subsystem, and (4) the control computer subsystem. The system configuration is shown in Figs. 2–4.

2.1. The Microscope and the ITV Camera Subsystem

The NICON microscope used here offers capabilities for transmitted and reflected lights which are convertible to each other by a switch. The basic parts of the microscope are, (a) the objectives, (b) an ocular without an eyepiece graticule, (c) a mechanical stage with sensers and a stage counter of X, Y, Z-coodinates for the stage location, (d) a monochromatic ITV camera, and (e) a monochromatic (B/W) monitor.

The objectives most commonly used are the $10\times$, $40\times$, $60\times$, $100\times$ and $200\times$ dry objectives, which are acceptable at both modes of transmitted and reflected light. The ocular of $10\times$ is fixed. Total magnifications are between $500\times$, $2,000\times$, $3,000\times$, $5,000\times$, and $10,000\times$ on the R.G.B.W. monitor in the image-processing subsystem, as listed in Table 1, on which identification and measurement of FTs is carried out.

The mechanical stage was modified with handmade reduction gear-boxes attached to the driving shafts. The locational data of the stage can be monitored on the stage counter. This data is collected by encoding units mounted on the shafts of the X, Y-traverse and another one mounted directly on the fine focussing knob for Z-vertical motion, as shown in Fig. 5. Positional resolution and repeatability for the Z-vertical motion are correspondingly accurate enough in the interval of $0.2\,\mu m$ per digit. On the other hand, the accuracy of measurements of the X, Y-traverse is in the interval of $2\,\mu m$ per digit
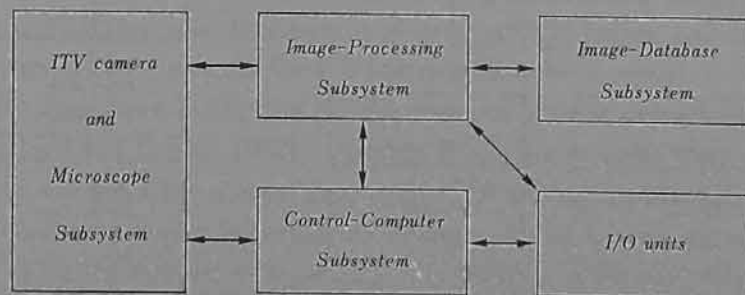

Fig. 2. Current system configuration of the computerized image-processing system for FT dating (CIPS-FTD).
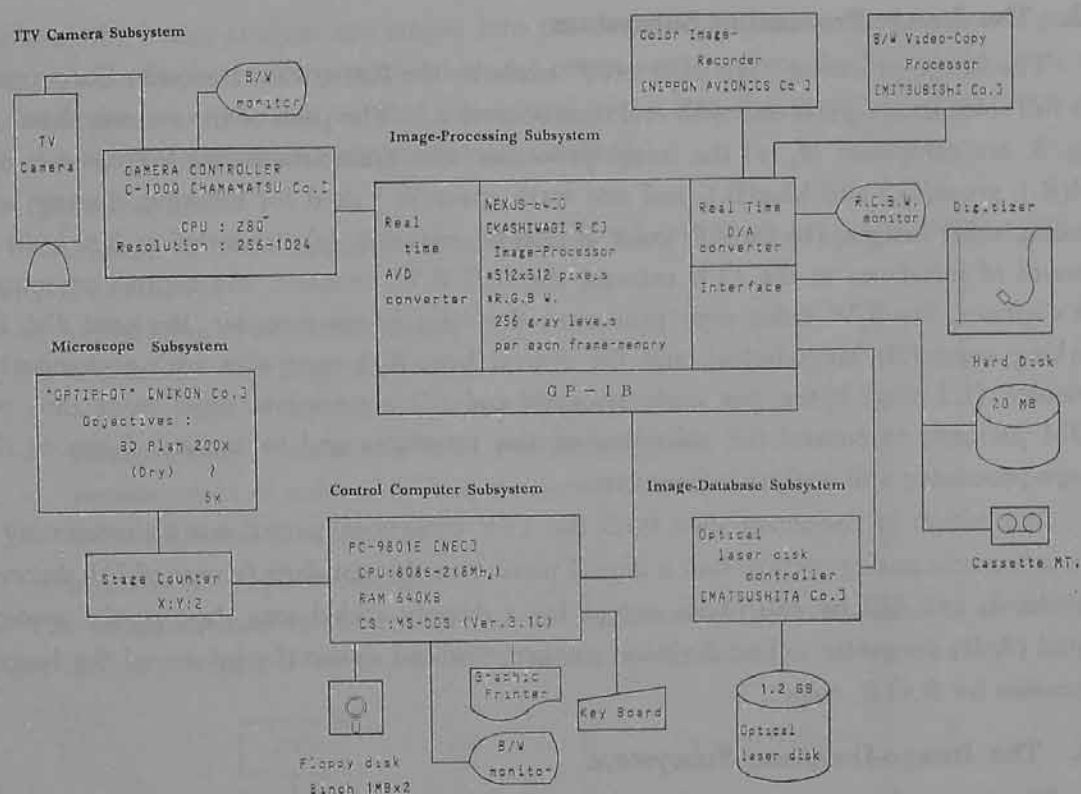
ITV Camera Subsystem

Fig. 3. Illustration of the hardware units of the computerized image-processing system for FT dating (CIPS-FTD).

Table 1. Values of the microscope magnification, screen size and resolution to each objective on the R.G.B.W. monitor. The ocular of $10 \times$ is fixed.

Ocular	Objectives	Magnification	Screen Size (μm)	Resolution per pixel (μm)
$10\times$	$10\times$	$500\times$	400×400	0.83×0.83
"	$40\times$	$2,000\times$	100×100	0.21×0.21
"	$60\times$	$3,000\times$	67×67	0.14×0.14
"	$100\times$	$5,000\times$	40×40	0.08×0.08
"	$200\times$	$10,000\times$	20×20	0.04×0.04

enough for the identification and location of the objective sample but not enough for the quantitative measurement of FTs. Operation of the mechanical stage is driven and controlled manually by the operator in the usual way looking at the X, Y, Z-coordinates of the stage location on the stage counter.

The monochromatic ITV camera using a sensor "Chalnicon tube" can now collect the images of the pattern of FT distribution with a high resolution power of 700 lines. The images are monitored on a high-resolusion analog B/W monitor in real time to the microscope operation.

2.2. The Image-Processing Subsystem

The image-processor "NEXUS 6400" made by the KASHIWAGI Research Corporation is a full color image-processor with real time operation. The parts of the system, shown in Fig. 3, are composed of, (a) the image-processor with frame-memories for three colors, red(R.), green(G.) and blue(B.), and one work space(W.) used for masking, tracing, and framing color images, (b) the full color R.G.B.W. monitor, (c) the interface box built in a series of interfaces to the ITV camera, the R.G.B.W. monitor, the control computer, the digitizer, the B/W video-copy processor, the color image-recorder, the hard disk for working space (20 Mega-bytes), and the optical laser disk controller with a changeable cartridge (1.2 Giga-bytes per each volum), and (d) connection cases built into the ROM packages to control the softwares of the interfaces and to command sets of the image-processing and analyzing functions.

Acquisition of the image-data from the ITV camera is carried out by converting a monochranatic analog picture into a digital picture in the standard format of 256 discrete gray levels and 480 by 480 pixels except for a density scaled area through the analog/digital (A/D) converter. The digitized picture is stored optionally in one of the frame-memories for R.G.B. colors.

2.3. The Image-Database Subsystem

The image-database subsystem as one of the main elements of the CIPS-FTD consists of an optical laser disk controller with a changeable cartridge shown in Fig. 6., and hierarchical type image-database management software. The optical laser disk controller having 1.2 Giga-byte memories characterized by add-write/read functions can store 5,546 monochromatic digital pictures or 1,848 color digital pictures per volume. This capacity is enough for normal FT dating procedures and is sufficient for the purpose of the construction of a computer-assisted instruction (CAI) system to educate beginners.

2.4. The Control Computer

The controls of the CIP-FTD are carried out through the control computer which is a very common personal computer, such as those made by NEC, IBM, or APPLE. All of the application programs are written in the BASIC language using the command sets of the image-processor, which make it possible to maintain easy communication with the system in an interactive mode. The functions of handling, storing, retrieving and analyzing the FT image-data have been realized flexibly by selecting menues with keying or digitizer pointing.

3. Procedures for the Application of the CIPS-FTD

3.1. A Procedural Model and the Logical Structure

The digital pictures collected at any stage and subjected to measurement procedures are automatically arranged and stored in the image-database. The numerical data as the

results of the image-analysis are stored into the numerical database in the control computer. Accordingly, if the procedural model corresponds well to the logical structure of the databases, it is possible to read procedural views into the structural description of both the image-database and the numerical database.

(1) *Procedural Model*

The model of the measurement procedures for FT dating by the CIPS-FTD is described as follows;

    a. registration of objective grains,

    b. evaluation of etching conditions,

    c. measurement of three-dimensional FT patterns,

    d. measurement of induced FTs in a re-etched grain,

    e. measurement of induced FTs in a external detector,

    f. calculation and presentation.

(2) *Structure of the Logical Database*

The image-database management system implimented here is classified as a kind of tree structure which is composed of a hierarchy of elements, called "nodes". The
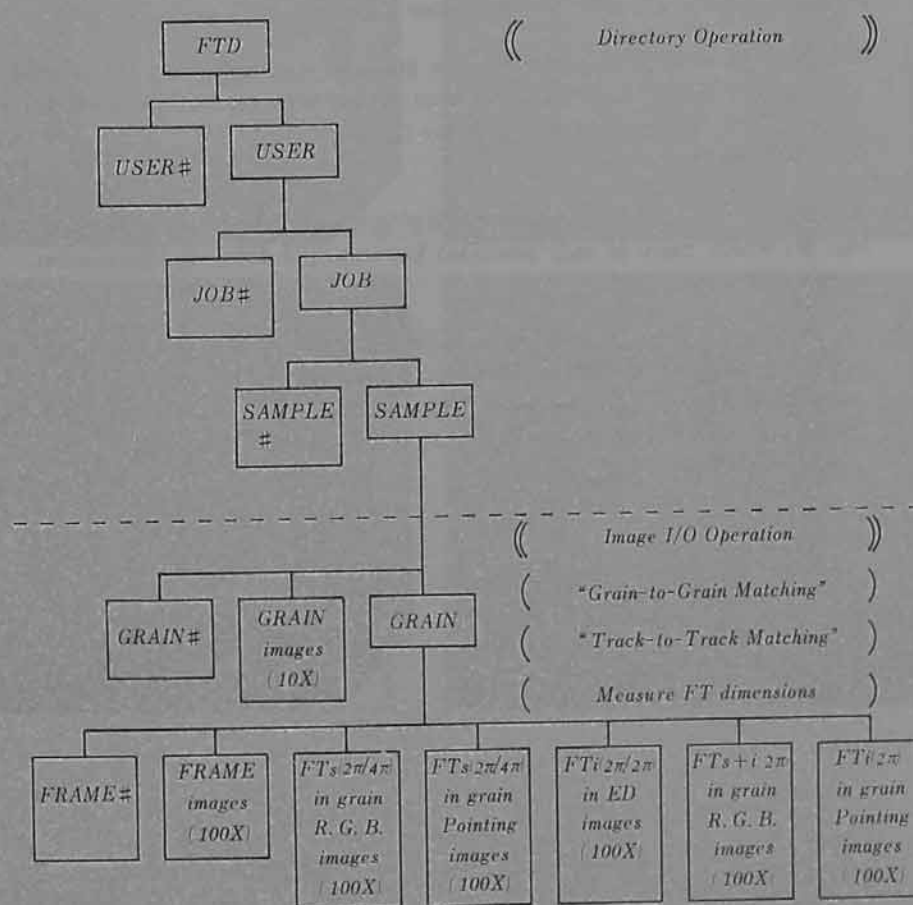
Fig. 7. The logical data structure of the image-database classified as a tree structure with hierarchical elements.

Fig. 4.   A photograph of the CIPS-FTD, with the microscope subsystem on the right, the image-processing subsystem; the R.G.B.W. monitor in the center, and the processor in the cabinet on the left. The optical laser disk controller with a changeable cartridge (1.2 Giga-bytes per each volume) is in the same cabinet on the left, and the control computer is in the center.

Fig. 5.   The mechanical stage modified by handmade reduction gear-boxes attached to the driving shafts. X,Y,Z-coordinates are collected by the encoding units mounted on the shafts and directly mounted on the fine focussing knob. The coordinates can be monitored on the stage counter.

Fig. 6.   The optical laser disk controller with a changeable cartridge of 1.2 Giga-byte memory, characterized by add-write/read functions. It can store 5,546 monochromatic digital pictures or 1,848 color digital pictures per cartridge.

Fig. 8.   A registered microscopic picture of a grain in a sample with the objective of $10 \times$, on which the registered key values are superimposed at the lower left-hand corner of the picture used to search for the objective grains. The screen size is 400×400 μm.

Fig. 9.   An integrated picture of 64 grains belonging to one sample resulting from searching, on which there is only principal key enlarged for easy observation. The screen size is 400×400 μm.

Fig. 10.   A suitable area for measurement with reference to FT distribution outlined with the polygon-framed area including more than four points. The framed area is displayed with the work frame-memory (W) overlapping the R.G.B. pictures. The screen size is 30×30 μm.

4

5

6

8

9

10
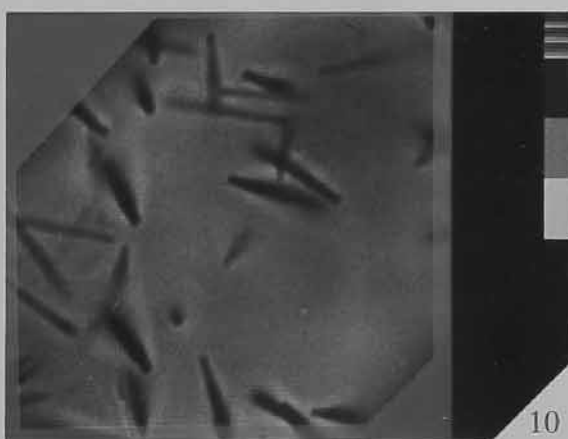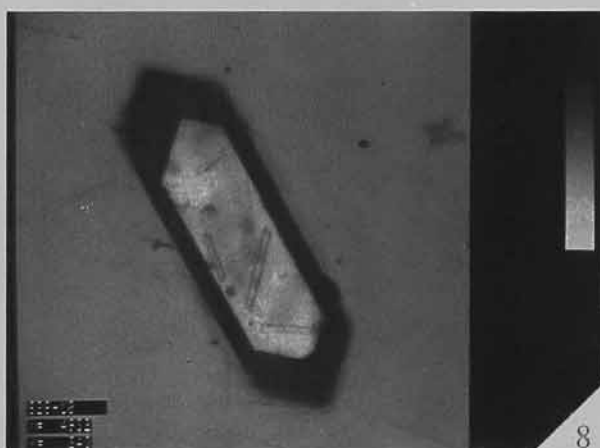
Fig. 11.   Explanation pictures of "track-to-track matching". Before strict adjustment, a picture has blurred color images on the R.G.B.W. monitor with both the pre-stored picture in red and the collected picture in green coming from the ITV camera in real time.   The screen size is 30×30 μm.

Fig. 12.   The blurred images of FTs on both pictures change to a single sharp yellow color by adjusting their locations.   The locational accuracy confirmed between the two pictures is less than 0.1 μm.   The screen size is 30×30 μm.

Fig. 14.   Pictures of multi-density FT images in 256 discrete gray levels taken on the zircon "step-etched" for two hours in KOH-NaOH eutectic at 230°C (Gleadow et al. 1976) for a total of 46 hours.   The zircon is a prospective age standard, named JVST24, collected from the Usunaka moonstone rhyolite welded tuff, Toyama Prefecture, central Japan.   The K-Ar age was reported to be 24 m.y. by Yamasaki et al. (1970) and the FT age to be 23.7 m.y. by Ganzawa (1983). The screen size is 30×30 μm.

Fig. 15.   Pictures of binary-density FT images converted from multi-density FT images.   The screen size is 30×30 μm.

Fig. 16.   A zoned color picture of the growing FT images.   The screen size is 30×30 μm.

Fig. 17.   A stereo-contour map of edge lines of the growing FT images by "step-etched", drawn by the X-Y plotter.   The higher contours are the edges of earlier FT images and the lower contours are that of later FT images.

11

12

14

15

16

17
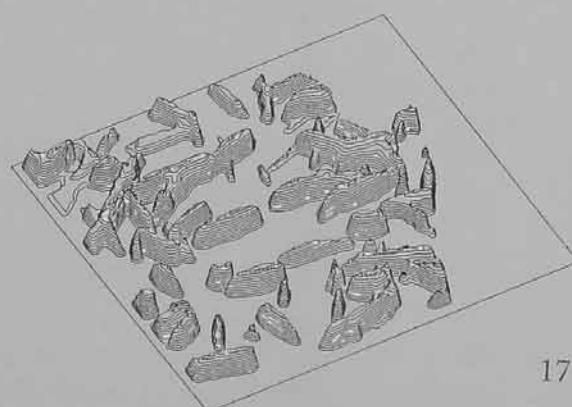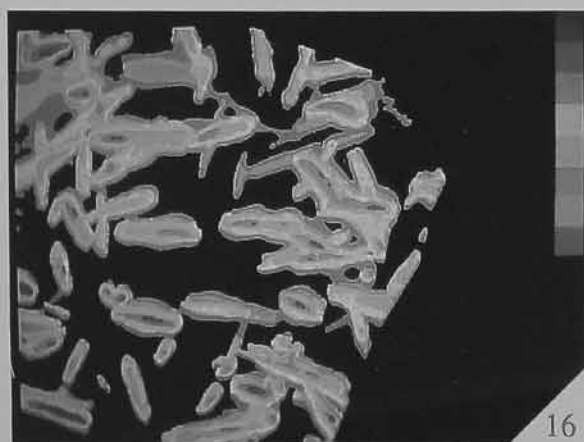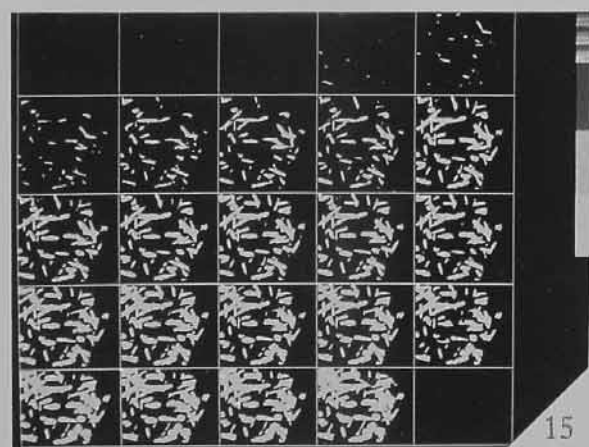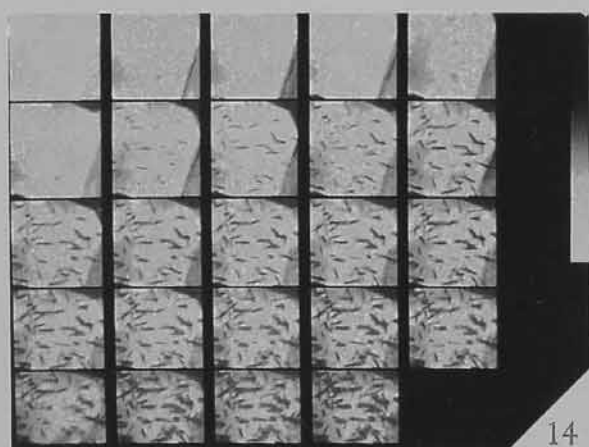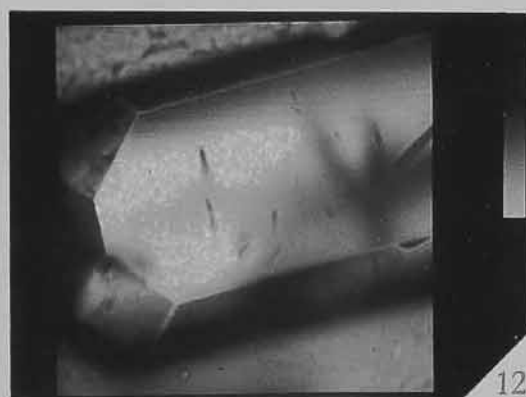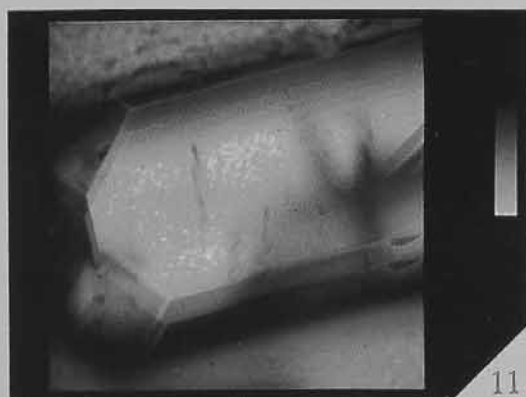
uppermost level of the hierarchy has only one node, called "the root". Elements at the end of the branches are called "leaves" in which image-data is stored. Except for the leaves, the hierarchical elements are searching keys which are used to uniquely identify the leaves. The overall view of the image-database is shown in Fig. 7. as that of the logical-tree structure.

On the other hand, the logical structure of the numerical database is in the line of the relational database. This is composed of four flat files, as referred to as relations; GRAIN, FRAME, ETCH and FT3D. Each relation consists of following domains;

GRAIN (SAMPLE♯, GRAIN♯, LOC (X, Y), SORT, MAX-LENGTH, MIN-LENGTH, AREA, AZIM-ANGLE)

FRAME (GRAIN♯, FRAME♯, AREA, SORT-FT, FT-COUNT)

ETCH (FRAME♯, FT♯, CENTR-LOC (X, Y), AZIM-ANGLE, APP-LENGTH, WIDTH)

FT3D (FRAME♯, FT♯, PIT-LOC (X, Y), DIP-ANGLE, AZIM-ANGLE, APP-LENGTH)

Those relational files are in active in the control computer.

3.2. Registration of the Grains

(1) *Arrangement of the Key Values*

Grains of each sample are put in order in a matrix (100×100 grains) on translucent PFA Teflon. All of the information about the objective samples and grains is described and registered in the image-database. This information will be combined with all of the other data collected later and structured. To register each objective grain, the searching keys; a user-code, a job-code, a sample-code, a grain-code and X, Y-coordinates of the microscope stage, are defined.

(2) *Collection of Grain Pictures for Registration*

We take the microscopic digital pictures of the grains in a sample with the objective of $10\times$ and superimpose the key data as an image at the lower left corner of each digital picture of the grain, shown in Fig. 8. These pictures are stored in the image-database for registration.

(3) *Query Operation to the Image-Database*

It is often necessary to search the image-database in order to find the pre-stored digital picture with multiple keys, referred to as "finding the sample node". The operation to fix the sample node is called the "directory operation". After the directory is fixed for only one sample, storing and searching operations for any digital picture are executed in real-time response. A digital picture or a set of 64 pictures in a matrix (8×8 subrfames) which is the result of searching, is displayed on the R.G.B.W. monitor, shown in Fig. 9.

(4) *The "Grain-to-Grain Matching" Method for the Operation of the Microscope*

One of the most important operations of the system, so called "grain-to-grain matching", is very effective in repeatedly setting an objective grain under the microscope.

The method of "grain-to-grain matching" requires steps, such as searching and displaying the digital picture of the objective grain, referring the key data about the grain, and manually setting the objective grain under the microscope in accordance with the X,Y-coordinates. The grain is confirmed by comparing it with the registered picture on the R.G.B.W. monitor and to the picture on the B/W monitor which comes directly from the ITV camera on the microscope.

(5) *Analysing the Shape of the Objective Grains*

The factors examined in the analysis of each grain are, (a) the maximum length, (b) minimum length, (c) area, and (d) the angle of inclination of the c-axis to the base line X. There are two kinds of the analytical methods. One is a fully automated analysis using the system function by image-analysis, and the other is an interactive measurement using the digitizer. All data is stored in a floppy file of the control computer.

3.3. Evaluation of the Etching Conditions

After etching, FTs in the objective grain grow so as to be observable under a microscope. Since the differences in material, crystallographic orientation and etching time influence the efficiency of revealing FT, it is essential to evaluate the optimum etching condition in order to obtain reliable data. This is done by using the following procedures:

(1) *Collecting Digital Picture and Defining Framed Area for Measurement*

Microscopic digital picture with the objective of $100\times$ is taken and observed on the R.G.B.W. monitor. In order to fix the suitable measurement area with reference to FT distribution, the outline with the polygon-frame including more than four points is interactively defined by the user with the digitizer, as shown in Fig. 10. The framed area is overlappingly displayed with the work frame-memory(w) upon the color picture in the R.G.B.W. monitor. A numerical value of it's area is automatically calculated and stored in a floppy file of the control computer. On the other hand, the digital pictures of both the FT images and the polygon-frame are also stored in the image-database. They are frequently used in the following procedures.

(2) *The "Track-to-Track Matching" Method for the Operation of the Microscope*

When repeatedly collecting digital pictures of the same objective area, the method for the microscopic operating, called "track-to-track matching", can be used. It contains the following steps: Display the pre-stored digital picture of the FTs in red on the R.G.B.W. monitor; Putting the grain under the microscope by the "grain-to-grain matching" method described before, continuously taking the microscopic pictures with the objective of $100\times$; Displaying them on the R.G.B.W. monitor in green, and moving the green picture manually by controlling the stage of the microscope, as shown in Fig. 11. In this way, the blurred images of FTs on both pictures change to a single sharp yellow color by adjusting their location, as shown in Fig. 12. The locational accuracy confirmed between the two pictures is less than 0.1 μm.

(3) *Converting a Multi-density Digital Picture into a Binary One*

The digital pictures of the FT images have a density of 256 discrete gray levels, as
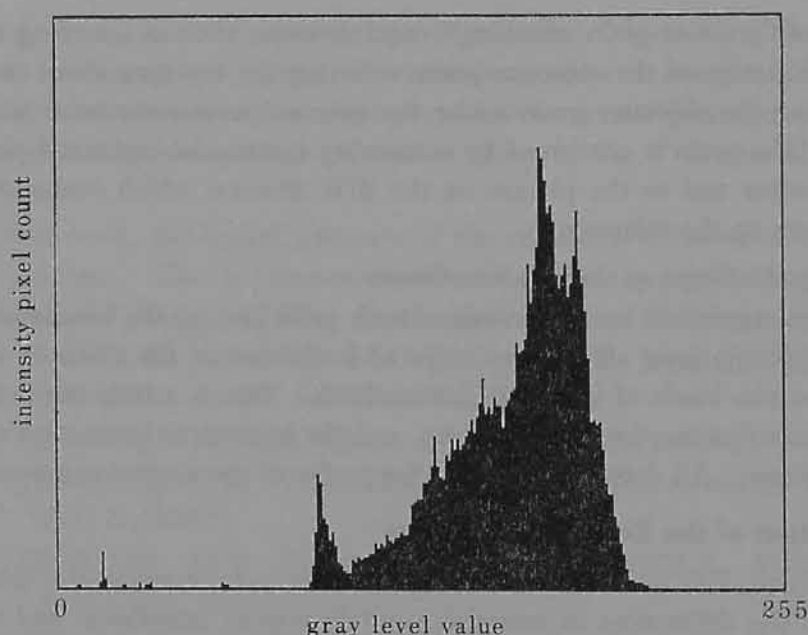
Fig. 13.   Density histogram as a graph plotting the distribution of the densities of all
picture elements in 256 gray levels.   This is very useful for conversion to a
binary picture.

Table 2.   After conversion, the binary picture is revised using the
revising commands of the system.

◎REJECT ......rejection of images on the frame boundary.
◎HFILL ....filling of absent dots of holes in images.
◎EROS ....erosion of images.
◎DILA ....dilatation of images.
◎ELIM ....elimination of small noisy dots

---

shown in Fig. 14.   Watching the density histogram as a graph plotting the distribution
of densities of all picture elements, as shown in Fig. 13, we can interactively convert it
into a binary picture, as shown in Fig. 15.   After conversion, the binary picture is revised
using the revising commands of the system, listed in Tab. 2. these are controlled by se-
lecting the option menues.

Subtraction between just the same digital pictures, even if there are many inclusions,
scratches and rims in them, leads to a picture in containing little or no density distribu-
tion.   Therefore, the digital pictures were taken in the "step-etched" procedures; the
earliest picture (M0) and the later pictures (M1).   The subtraction (M1-M0) made the
picture (Ms) with only new growing FT images in the black background.   The contrast
between FT images and the background was very high that it was very easy to extract the
binary FT images.

(4)   *Extracting the Characteristics of FTs*

In order to obtain characteristic images of the growing FTs, edges and skeltons are
extracted from the FT images by using the commands, listed in Tab. 3, which are built

Table 3.   The commands of edging and skelton.

◎EDGE ....edging of images.
◎THIN ....skeltonization of images.

Table 4.   The commands for quickly counting FTs by means of the
EULER method and for steadily numbering each FT by
the labelling operation.

◎EULER.........fast grain counting (EULER method).
◎LABEL.........labelled counting to all of FT images ($\leq$6143).

Table 5.   The commands to analyse each labelled FT image and to
obtain a series of numerical values about FT dimensions.

◎ANALY .... analysis with options; A-L, default; all.

A :	XMAX (horizontal maximum width)
B :	YMAX (vertical maximum width)
C :	CXMAX (horizontal length)
D :	CYMAX (vertical length)
E :	perimeter
F :	area
G :	co-ordinate of centroid (X1, Y1)
H :	MAX (maximum length)
I :	θ (inclination to the base line X)
J :	MIN (minimum length (vertical to H))
K :	co-ordinates of H (X1, Y1, X2, Y2)
L :	co-ordinated of J (X1, Y1, X2, Y2)

---

into the application program.   A series of the images, the results of edging the pictures collected on the "step-etched" grain were also superimposed.   The overall results of this processing are shown in both Fig. 16–17.   With these figures, it is easy to view growing FTs as time for etching passes.

(5)   *Counting the Number of FTs*

Using the commands listed in Tab. 4, FTs can quickly be counted by means of the EULER method, and each FT can be numbered by a labelling operation which is accessible up to 6,143 tracks per picture.

(6)   *Measuring the Numerical Values of FT Dimensions*

Each labelled FT image is analysed to obtain a series of numerical values about the FT dimensions, as shown in Fig. 18, by using the command with the functions described in Tab. 5.   The resulting numerical data is stored in a floppy file of the control computer and used for the evaluation of etching conditions.

(7)   *Evaluation of the Results*

A sufficiently large amount of numerical data is collected enough to reliably calculate the FT age of a sample.   However, the proceeding analysis based on only one digital

Fig. 19–23.   The digital pictures taken at the stepped range, downward of the micro-
scope's focussing points on the same framed area of the objective zircon used
to collect the three-dimension FT patterns.   The DP-1, DP0, DP1, DP2 and
and DP3 are shown from Fig. 19 to Fig. 23.   The screen size is $30 \times 30 \ \mu m$.

Figs. 24–26.   Three pictures (DP0, DP1, DP2) sharpened with five pictures (DP-1, DP0,
DP1, DP2, DP3) taken at stepping focus points.   The moving distance of a
step is 1.6 μm per 8 digits or 3.2 μm per 8 digits in zircon minerals in order to
correct the refractive index, 1.99.   The step distance is changeable with re-
ference to the FT length.   The screen size is $30 \times 30 \ \mu m$.

Fig. 27.   The relation between color ranges and their lengths.
A dip angle (θ);
    $\tan \theta = d/OA' = 2.0 \ d/OB'$
        d   ; the moving distance of the focus,
        OA' ; the distance from a yellow starting point (O) to a yellow and
                magenta boundary point (A'),
        OB' ; the distance from the starting point (O) to a magenta and cyan
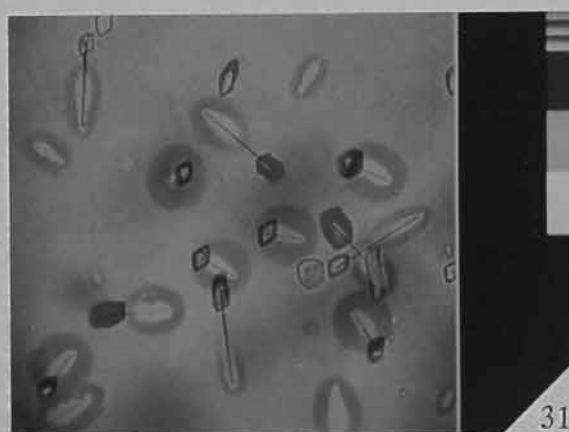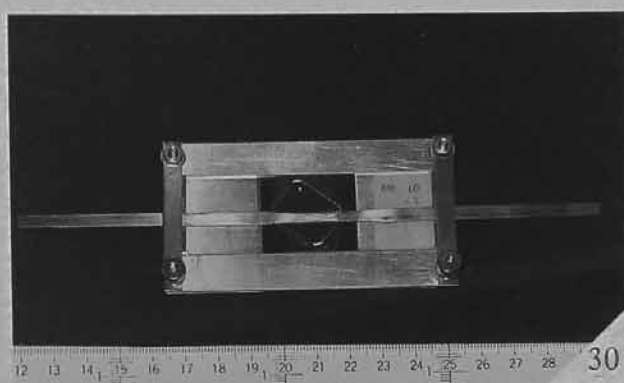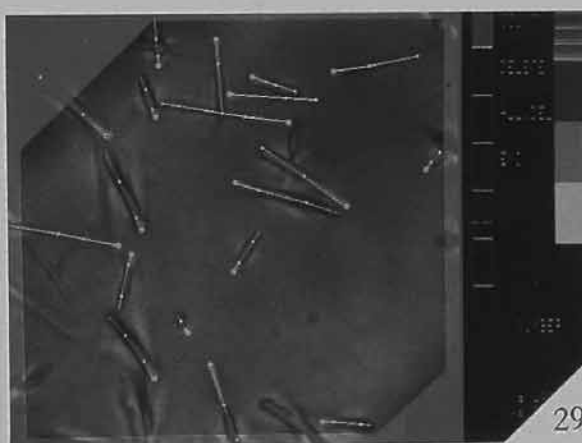   boundary point (B').
A real length (OC);
    $OC = OC'/\cos \theta$
        OC' ; the distance from the starting point (O) to a cyan end point.

19

24

20

25

21

26

22

27

23

Fig. 28. A stereographic colored picture displayed on the R.G.B.W. monitor using DP0, DP1 and DP2 with colors of blue, green and red in reverse order. Three-dimensional informa·ion is in a range of colors; yellow at the near etch-pit, magenta in the middle and cyan at the tail. The screen size is 30×30 μm.

Fig. 29. Pointing procedures displayed with tiny circles and lines upon the stereographic colored FT picture, using the work frame-memory (W). The screen size is 30×30 μm.

Fig. 30. The handmade special holder, on which adjusting the initial position of the mounts, the sample and the detector, was carried out with the pin pricks or image-matching under the microscope.

Fig. 31. The mass of the induced FTs in the detector correlated to the paired FTs in the standard glass, NBS SRM612. The screen size is 30×30 μm. The sample was irradiated at the Kyoto University Reactor (KUR).

28

29

30

31

```
-------------------------------------------------------------------------
                NUMBER OF TRACK             =   12
-------------------------------------------------------------------------
    No.     CENTROID       LMAX          CO-ORDINATE             THETA
            CX     CY              MX1    MY1    MX2    MY2      (DEG)
-------------------------------------------------------------------------
     1      151    242      19    161    242    142    244         6
     2      409    291      13    411    298    408    285       103
     3      228    317      30    241    309    216    327        36
     4      264    323      17    267    332    262    315       106
     5       70    354      48     94    349     46    358        11
     6      238    362      72    274    370    203    357       170
     7      145    409      50    170    403    121    414        13
     8      337    444      17    343    452    330    440       137
     9       59    460      57     85    452     30    469        17
    10      244    455      66    278    453    212    458         4
    11      360    469      26    370    477    351    459       137
    12      245    474       8    248    471    242    477        45
```

Fig. 18. A computer output list of numerical data that resulted from the image-analysis
         by the command "ANALY", as shown in Table 5. They are stored in a
         floppy file of the control computer and used for the evaluation of the etching
         condition.

picture is not enough to separate the objects such as track-in-track, track-in-cleavage
and dislocation. This means that collected results are mixed and not pertinent to the
calculation of FT ages, but they are useful for the evaluation of the relative changes in
dimension or density of FTs.

3.4. Measurement of the Three-dimensional FT Patterns

The information contained in many types of pictures are basically two-dimensional.
On the other hand, it is necessary to know the three-dimensional FT patterns by progres-
sive research. It seems to be very difficult to extract the three-dimensional data from a
picture. Thus, an attempt was made to obtain a series of digital pictures taken at the
stepped range of focussing points of the microscope, and to analyze them to extract ster-
eographic information.

(1) *Collecting Digital Pictures at Several Focussing Points*

The microscopic operation, called "track-to-track matching", should be done on one
of the framed areas of an objective zircon grain in a sample. The operation of collecting
the microscopic pictures with the objective of $100\times$ may be divided into the following
stages (a~f):

   a. Put the focus at the real surface of the grain which is recognized by the reflective microscopic observation, and reset the digital counter for the Z-axis movement to zero.

   b. Move the focus upward to the digit 4, and take a picture there (DP-1, shown in Fig. 19).

   c. Move the focus downward again to the digit 0, and take a picture (DP0, shown in Fig. 20).

   d. Move the focus forward to the digit 8, and take a picture (DP1, shown in Fig. 21).

   e. Repeat twice to the digit 16 and digit 24, and take pictures (DP2 and DP3, shown in Figs. 22–23).

   f. All of these results are stored in a work image-file on the hard desk.

(2) *Sharpening Blurry Pictures*

Sharp unblurred pictures are desired, but each picture has a blur due to diffusion. In order to obtain unblurred pictures, subtract a positive multiple of its Laplacian (ROS-ENFELD and KAK, 1982). This is one of the most popular image-processing operations. Suppose that DP0 has blurry images from both the upper DP-1 and lower DP1. The unblurred DP0 is obtained by subtracting a Laplacian of DP-1 and DP1. The same procedures are taken on two sets of DP0·DP1·DP2 and DP1·DP2·DP3. As a result, the three unblurred digital pictures; DP0, DP1 and DP2, as shown in Figs. 24–26, which are at the focussing points of 0, 8 and 16 can be collected. The moving distance of the focus is just $0.2\,\mu m$ per digit, $1.6\,\mu m$ per 8 digits or $3.2\,\mu m$ per 8 digits in zircon in order to correct the refractive index, 1.99 experimentally confirmed. This should be change with reference to the length of FTs; longer in apatite and shorter in thermal annealing minerals.

(3) *The Stereographic Presentation with Colored FT Images*

The three unblurred digital pictures (DP0, DP1, DP2) are stored in the image-memories for colored images of blue, green and red in the reverse order. This means that a composite color picture is displayed on the R.G.B.W. monitor. The three-dimensional information can be easily extracted from the colored FT images, on which just focussing parts of FT images are very dark, so that the color of the DP0 becomes yellow (R.+G.), DP1 becomes magenta (R.+B.) and DP2 becomes cyan (G.+B.), as shown in Figs. 27–28.

(4) *Measurement and updating the Three-dimensional FT Patterns*

We shall now illustrate, as shown in Fig. 27, how the stereographic dimensions can be calculated. A dip angle of a track(θ) is defined by the equation

$$\tan \theta = d/OA' = 2.0\ d/OB'$$

where   d   ;   the moving distance of the focus,

         OA' ;   the distance from a yellow starting point (O) to a yellow and magenta boundary point (A'),

OB' ;   the distance from the starting point (O) to a magenta and cyan bound-
        ary point (B').

A real length of a track (OC) is defined by the equation

$$OC = OC'/\cos \theta$$

where   OC' ;   the distance from the starting point (O) to a cyan end point.

Using the stereographic colored pictures, the locations of points on an FT image
are interactively measured with the digitizer, (O) a yellow starting point, (A') a yellow
and magenta boundary point, (B') a magenta and cyan boundary point, and (C') a cyan
end point. For a short or a gently dipping track, the operation is interrupted by default
and ends before the end point. Based on the X,Y-coordinates of the points, the system
calculates not only the number but also the dips, azimuth angles, and apparent and real
track lengths.

For the track colored only in yellow with no point A', the dip angle (θ) can not
measure, but it is so small that the apparent length is nearly equal to the real length of
the longer FTs, which will be in the zone A on the Fig. 35. For the track colored from
yellow to cyan in the form of spots, the dip angle (θ) should be vrey high near vertical
and it is difficult to measure precisely both dip angle and length, they will be in the zone
C on the Fig. 35, in which the data in both zones A and C were omitted. In the new
program version, the colores range from white, yellow, magenta to cyan. The first
moving distance becomes d/2 (about 1.6 μm) and the difficulty in the zones A on the
Fig. 35 have been overcome. Also the difficulty in zone C have been solved. The details
will be reported in the near future.

All measurement procedures are displayed as pointing images with tiny circles and
lines, which overlap each FT image, as shown in Fig. 29. Using these images, opera-
tions of addition, deletion, and replacement of FT data can be done at any time in the
procedures. All of them are stored in the image-database and used for the evaluation
and maintence of FT data.

(5) *Recognizing and Separating FTs from FT-like Objects*

A real FT has a yellow colored etch-pit, so it is possible to easily separate the over-
closing FTs, track-in-track or track-in-cleavage by using the yellow spots of the etch-
pits. Finally, there are still some FTs in question. These should be checked by com-
paring them with changing images on the B/W display by moving the stage of the micro-
scope.

3.5. Measurement of Induced FTs in the Re-etched Grain

Measuring induced FTs in the re-etched grain, the same operational procedures, de-
scribed above, are used to collect a stereographic colored picture of the FTs mixing both
spontaneous and induced FTs. When measuring the induced FTs, use the old masking
images of both the polygon-frame and the measurement point tracing which were col-
lected during the measurement of the spontaneous FTs in the same area. Measure the
induced FTs on which no point tracing images are found, and extract only the new FTs
as the induced FTs.

3.6. Measurement of the Induced FTs in the External Detector

One of the difficulties in the external track detector method is to map grain locations and their equivalent sites on the external detector. The careful adjustment and counting of the induced FTs in the external detector by the operations have been successfully done, as mentioned in the next paragraphs.

(1) *Adjusting the Mounts Using Pin Pricks*

The procedure of adjusting and setting the initial position of the mounts, the sample and the detector, is first carried out using the pin pricks at the four corners of the mounts. The special holder, shown in Fig. 30, is arranged so that it is possible to move the overlaid detector under the steroscopic microscope and adjust the pin pricks manually.

(2) *Adjusting the Mounts by Image-Matching*

The mounts under the microscope are carefully adjusted with the objective of $40\times$ or $60\times$, i.e. the images of both the grain and the related mass of the induced FTs are adjust very carefully by hand, monitoring the B/W display. This operation is repeatedly executed at the near corners of the mounts. After these operations were done, the mounts were fixed with pieces of soft adhasive tape and removed from the holder.

(3) *Collecting Back-side Pictures of Induced FTs*

First, the database is searched to obtain the digital picture which was used to count spontaneous FTs and dispaly them on the R.G.B.W. monitor in red color. On the other hand, the fixed mounts were put under the microscope with the objective of $100\times$, the focus was first set on the surface of the grain, and digital pictures which came directly from the ITV camera on the microscope, were continuously displayed on the R.G.B.W. monitor in green color. Adjustment of the two color images is possible by using the "track-to-track matching" method. In the next step, the focus is changed upward on the detector, and a digital picture of the induced FTs is collected from the back of the detector. This picture is very useful in guiding the relational location, but it is not suitable for directly counting tracks because of its low resolution. Much more careful matching should be done by using both the vertical induced FTs in the re-etched grain and the registered induced pair of FTs in the detector, as shown in Fig. 31. We store this digital picture in the image-database after turning it over from left to right by the "mirroring operation".

(4) *Fixing the Detector on a Slide Glass*

A slide glass covered with bifacial adhesive tape on the lower side, is prepared and brought down very slowly and carefully on the grain mount slide at the same position of both slides. After that, the detector is fixed on the upper slide.

(5) *Setting the Framed Area on the Detector*

Referring to the mirrored X,Y-coordinates, the mass of induced FTs in the detector can be easily put under the microscope by "grain-to-grain matching". Both the FT images of the digital pictures taken from the back and collected from the ITV camera are adjusted in the same relational location by the "track-to-track matching" method.

(6) *Counting the Induced FTs in the Detector*

In order to obtain the number of the induced FTs in the detector, it is possible to count the tracks based on a digital picture with the method used in the procedure for the evaluation of etching. However, if it is necessary to know the registering pair relationship between the induced FTs in both the re-etched grain and the detector, the procedure of measurement for the three-dimensional FT patterns should be taken as described in the previous paragraphs.

3.6. Calculation and Presentation

All numerical data collected by the above procedures were automatically stored in a floppy file of the control computer. By using the numerical data, a variety of the numerical values or graphs are developed by which evaluations of etching, fading, orientation and dating could be effectively done. The zircon used here was collected from the Harima granite, Hyogo prefecture, Southwest Japan (KISHIDA and WADATSUMI, 1967). The radiometric age by the Rb-Sr method is 79.5 m.y. (SEKI, 1978). The zircon etched in KOH-NaOH eutectic at 230°C for 16–20 hours. The data presented here is only that of the sponteneous FTs as before the report of system calibration. The spontaneous FT density is 5.22×10^6 (t·cm^{-2}).

(1) *Ages of a Sample*

The ages are calculated using two methods, i.e., (a) the external track detector method using both the external face (S2πES-I2πED: Age2πED) and the internal face (S4πIS-I2πED: Age2πED), and (b) other ages for very young samples are calculated by re-etch methods with both external (S2πES-I2πES) and the internal faces (S4πIS-I2πIS). The expressions in parentheses are based on Suzuki's classification (SUZUKI, M. 1984) and the author's simple representation.

(2) *Data and Diagrams for Fading Evaluation*

The data of this kind consists of, (a) lengths of the spontaneous FT on the external face: Ls2π, (b) lengths of the induced FT on the external or internal faces: Li2π, (c) the ratio of Ls2π/Li2π, and (d) the ratio of Age2πED/Age4πED. For fading evaluation, the diagrams of the spontaneous FT length (Ls2π) distribution are shown in Figs. 32–33 and 35.

(3) *Diagrams to Evaluate Orientational Efficiency*

The diagrams for evaluating etching efficiency against the crystallographic orientation are as follows; (a) a diagram of azimuth angle distribution to the C-axis, shown in Fig. 34, (b) a relational diagram for distributing both dip angle and length on a vertical section as shown in Fig. 35, and (c) a diagram of dip direction on the stereographic net with the N.S. poles coinciding with the C-axis, shown in Fig. 36.

4. Evaluation with Respect to CIPS-FTD Development

The following points can be considered in evaluating the system development; i.e.,
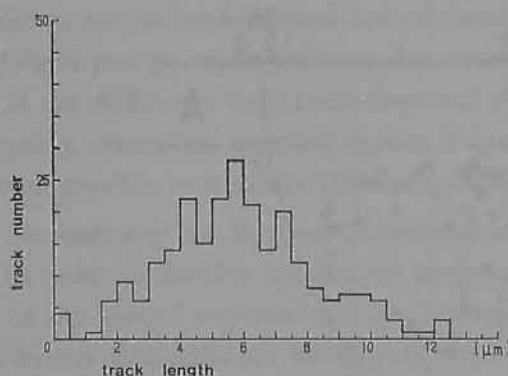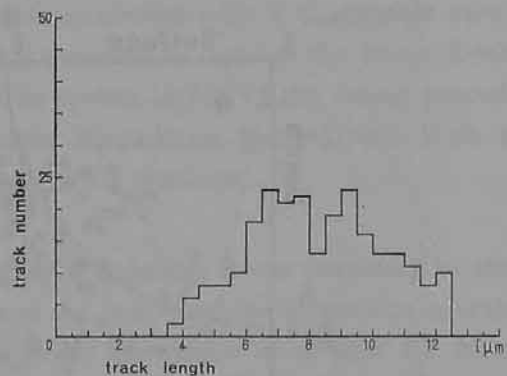
Fig. 32.

Fig. 33.

Fig. 32. A diagram of apparent length distribution of the spontaneous FTs in the external face of the zircon.

Fig. 33. A diagram of the real length distribution of the spontaneous FTs in the external face of the zircon.
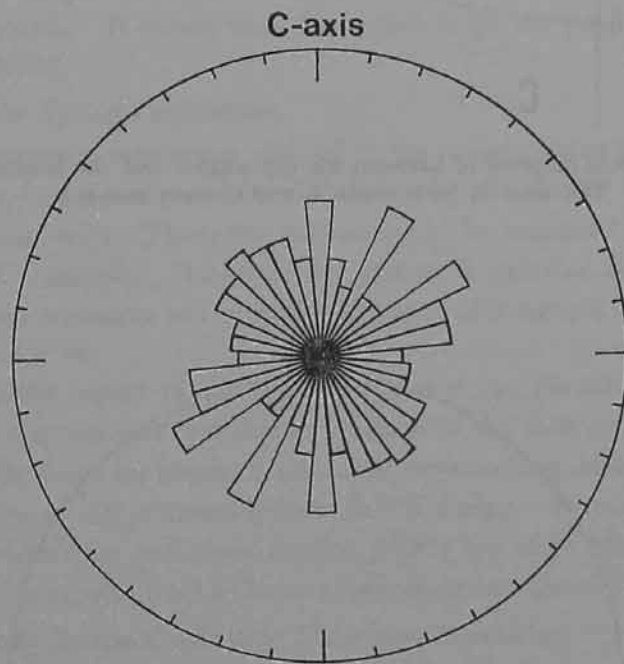

Fig. 34. A diagram of azimuth angle distribution to the C-axis excluding FTs dipping 80°–90°.

(a) the compositional hardware units, (b) software development, (c) system performance, and (d) system calibration.

(1) *The Compositional Hardware Units*

Most of the integrated hardware units are accessible to the market, but the interface cassettes, built in the basic control softwares, are only available from the Kashiwagi Research Corporation, the supplier of the NEXUS 6400 system. The fundamental configuration of the system is similar to the system reported by us at the international FTD workshop held in New York in 1984 (WADATSUMI and MASUMOTO, 1984). However, it
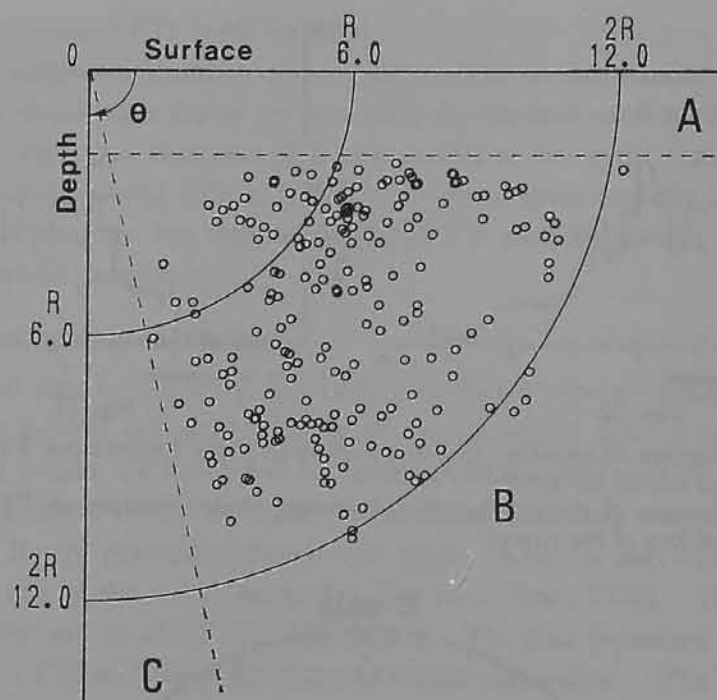
Fig. 35. A relational diagram of between the dip angles and the lengths in the vertical section. The data in both zones A and C were omitted.
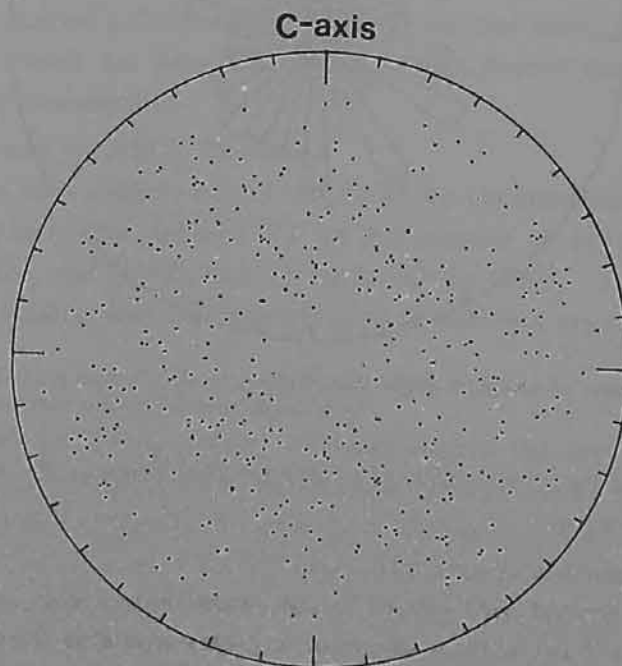

Fig. 36. A diagram of directional distribution of FTs on the stereographic net with the N.S. poles coinciding with the C-axis. The points in both left and right halves are in the relation of a point symmetry.

contains a newly implemented optical laser disk controller with a changeable cartridge (1.2 Giga-bytes per each volume) that makes it possible to develop the image-database. One of the difficulties in the development of the system is that in the dating procedures it requires enormous memory space, a hundred Mega-bytes per sample. With it, it becomes possible to measure the three-dimensional FT patterns.

(2) *Evaluation of the Software Development*

In order to develop application programs for FT dating, it was necessary to analyze both of the general experimental procedures and the man-machine interactive operations. This means that software developers require either knowledge of general FT dating or experience of computer system development. Though specialized systems for application to artificial intelligence still contain many difficulties, these were overcome to develop our system as a man-machine interactive system by which the user's intelligence becomes effective. Therefore, users of the system only need general knowledge and techniques for FT dating, but no knowledge of either the design or the programming of the computerized system. It means that the system helps the people who are operating in the field of FT dating.

(3) *Evaluation of the System Performance*

Many of the automatic operations realized in the measurement procedures make performance very high, but overall time for FT dating by the system is about one to three times that of the usual way. Thus, the system would be evaluated lower than if it only obtained the age of a sample. However, the system is valuable from another point of view, that the system measures not only the FT ages of a sample but also the three-dimensional patterns of FTs.

The most valuable aspect of the system is that it can permanently preserve all of the data, from the unprocessed raw digital pictures to the final numerical values of results. All of this data can be obtained and used for checking, deleting, adding and replacing at any time or at any processing point in FT dating. Because of those functions, the experimental techniques and their results, which are often closed and unavailable, could be opened to those who want to know more about and test the results of FT dating.

(4) *The Neccessity of System Calibration Using Age Standards*

The dependency of FT dating on age stadnards comes from ambiguous values of the ^{238}U spontaneous fission decay constant and the complexities of absolute neutron dosimetry. With either the $(\phi/\lambda f)$ or zeta calibration approach, it is inevitable that age standards be used at some stage. The use of age standards demands that calibrated ages be unambiguous and be reproducible in more than one laboratory and by more than one method.

The interlaboratory comparison of FTD techniques using age standards was done at the 4th International FTD Workshop held at Rensselaer Polytechinic Institute, Troy, New York in August, 1984 (MILLER *et al.*, 1985). The results of the interlaboratory comparison show that whereas the FT ages obtained by most analysts agree well with independent age standards, some others are in gross error. The above results stress that

there is a need for extensive and continued use of age standards in FT dating. Thus, it is necessary to calibrate the experimental procedures and dating ability of the CIPS-FTD using age standards. In the future, papers will be presented in which the zeta calibration values and the description of the three-dimensional FT patterns with reference to the age standards are discussed.

Acknowledgements

References

GANZAWA, Y. (1983): "Green tuff" movement defined by the fission track ages of igneous rocks Part 2 —The Futomiyama area of Toyama prefecture, central Japan— (in Japanese). Jour. Geol. Soc. Japane, 89, 271–286.

GLEADOW, A.J., HURFORD, A.J., and QUAIFE, R.D. (1976): Fission track dating of zircon: Improved etching techniques. Earth Planet. Sci. Lett., 33, 273–276.

HURFORD, A.J. and GREEN, P.F. (1982): A users' guide to fission track dating calibration. Earth Planet. Sci. Lett., 59, 343–354.

KISHIDA, K. and WADATSUMI, K. (1967): Volcanostratigraphy of the Himeji acid volcano-plutonic complex (in Japanese). Prof. H. Shibata Mem. Vol., 241–255.

MILLER, D.S., GREEN, P.F., HURFORD, A.J. and NAESER, C.W. (1985): Results of interlaboratory comparison of fission-track age standards: Fission-track workshop-1984. Nucl. Tracks, 10, 383–391.

ROSENFELD, A. and KAK, A.C. (1976): Digital picture Processing. vol. 1, 435, vol., 2, 349, Academic Press.

SEKI, T. (1978): Rb-Sr geochronology and petrogenesis of the late Mesozoic igneous rocks in the inner zone of the southwestern part of Japan. Mem. Fac. Science, Kyoto Univ., Series, geol. and min., 45, 71–110.

SUZUKI, M. (1984): Discussion on terminology, anisotropy, and interprocedural cross-checks of fission track ages on zircon. Jour. Geol. Soc. Japan, 90, 551–563.

YAMAZAKI, M., MIYAJIMA, Y. (1970): Eruption age of moonstone rhyolite in Toyama prefecture, central Honshu (in Japanese). Jour. Japan Assoc. Min. Petr. Econ. Geol. 63, 22–27.

WADATSUMI, K. and MASUMOTO, S. (1984): A potential applicatoin of computerized image-processing to fission-track dating by the re-etch method (Abstract). The Forth International Fission-Track Dating Workshop, Nucl. Tracks, 10, 436.

WATANABE, K. and ISHIBASHI, K. (1987): Dating of basalts by fission track method using zircon in xenoliths: application to basalts from Higashi-Matsuura Peninsula, Saga Prefecture, Japan (in Japanese). Jour. Geol. Soc. Japan, 93, 65–68.